inorganics

MDPI

Article

Synthesis and In Vitro (Anticancer) Evaluation of η^6-Arene Ruthenium Complexes Bearing Stannyl Ligands

Olivier Renier [1], Connor Deacon-Price [1], Joannes E. B. Peters [1], Kunsulu Nurekeyeva [1], Catherine Russon [1], Simba Dyson [1], Siyabonga Ngubane [2], Judith Baumgartner [3], Paul J. Dyson [4], Tina Riedel [4], Haleden Chiririwa [5] and Burgert Blom [1,*]

1 Maastricht Science Programme, Faculty of Humanities and Science, Maastricht University, Kapoenstraat 2, P.O. Box 616, 6200 MD Maastricht, The Netherlands; o.renier@alumni.maastrichtuniversity.nl (O.R.); c.deacon-price@student.maastrichtuniversity.nl (C.D.-P.); jeb.peters@student.maastrichtuniversity.nl (J.E.B.P.); k.nurekeyeva@student.maastrichtuniversity.nl (K.N.); c.russon@alumni.maastrichtuniversity.nl (C.R.); s.dyson@student.maastrichtuniversity.nl (S.D.)

2 Department of Chemistry, University of Cape Town, Rondebosch 7701, South Africa; siyabonga.ngubane@uct.ac.za

3 Institut für Anorganische Chemie, Technische Universität Graz, Stremayrgasse 9, A-8010 Graz, Austria; baumgartner@tugraz.at

4 Institut des Sciences et Ingénierie Chimiques, Ecole Polytechnique Fédérale de Lausanne (EPFL), CH1015 Lausanne, Switzerland; paul.dyson@epfl.ch (P.J.D.); tina.riedel@epfl.ch (T.R.)

5 Biosorption and Water Research Laboratory Department of Chemistry, Vaal University of Technology, Private Bag X021, Andries Potgieter Blvd, Vanderbijlpark 1911, South Africa; harrychiririwa@yahoo.com

* Correspondence: burgert.blom@maastrichtuniversity.nl

Academic Editor: Luigi Messori
Received: 13 June 2017; Accepted: 11 July 2017; Published: 13 July 2017

Abstract: Treatment of the known half-sandwich complexes of the type $[(\eta^6\text{-}C_6H_6)RuCl_2(P(OR)_3)]$ (R = Me or Ph) with $SnCl_2$ yielded three new half-sandwich ruthenium complexes (**C1**–**C3**): $[(\eta^6\text{-}C_6H_6)RuCl(SnCl_3)(P(OMe)_3)]$ (**C1**), $[(\eta^6\text{-}C_6H_6)RuCl(SnCl_3)(P(OPh)_3)]$ (**C2**) and the bis-stannyl complex $[(\eta^6\text{-}C_6H_6)Ru(SnCl_3)_2(P(OMe)_3)]$ (**C3**) by facile insertion of $SnCl_2$ into the Ru–Cl bonds. Treatment of the known complexes $[(\eta^6\text{-}C_6H_6)RuCl(SnCl_3)(PPh_3)]$ and $[(\eta^6\text{-}C_6H_6)RuCl_2(PPh_3)]$ with 4-dimethylaminopyridine (DAMP) and ammonium tetrafluoroborate afforded the complex salts: $[(\eta^6\text{-}C_6H_6)Ru(SnCl_3)(PPh_3)(DAMP)]^+BF_4^-$ (**C4**) and $[(\eta^6\text{-}C_6H_6)RuCl(PPh_3)(DAMP)]^+BF_4^-$ (**C5**) respectively. Complexes **C1**–**C5** have been fully characterized by spectroscopic means (IR, UV–vis, multinuclear NMR, ESI–MS) and their thermal behaviour elucidated by thermal gravimetric analysis (TGA). Structural characterization by single crystal X-ray crystallography of the novel complex **C2** and $[(\eta^6\text{-}C_6H_6)RuCl_2(P(OPh)_3)]$, the latter having escaped elucidation by this method, is also reported. Finally, the cytotoxicity of the complexes was determined on the A2780 (human ovarian cancer), A2780cisR (human ovarian *cis*-platin-resistant cancer), and the HEK293 (human embryonic kidney) cell lines and discussed, and an attempt is made to elucidate the effect of the stannyl ligand on cytotoxicity.

Keywords: bioorganometallic chemistry; metal-based drugs; phosphorus ligands; ruthenium; half-sandwich complexes; tin dichloride insertion

1. Introduction

Since the discovery of the anti-cancer properties of *cis*-platin, $[cis\text{-}PtCl_2(NH_3)_2]$ and related complexes [1–4], research directed towards the development of new metal-containing anticancer

drugs has made staggering advances [5–15]. Metals other than platinum are worth investigating in the search for new classes of metallodrugs with high efficacy and fewer side effects. The ongoing search for new metallodrugs has led to the discovery of several ruthenium-based drugs: NAMI-A and KP1019, both of which have completed phase I clinical trials, as well as RAPTA-C (Chart 1) [16–23]. In addition, ruthenium(II)-arene complexes are also considered promising drug candidates, owing to their demonstrated low toxicity and high antitumor activity [18–30]. The bioavailability of these compounds is controlled by the arene moieties facilitating the outreach in the intracellular region given their hydrophobic nature [29].

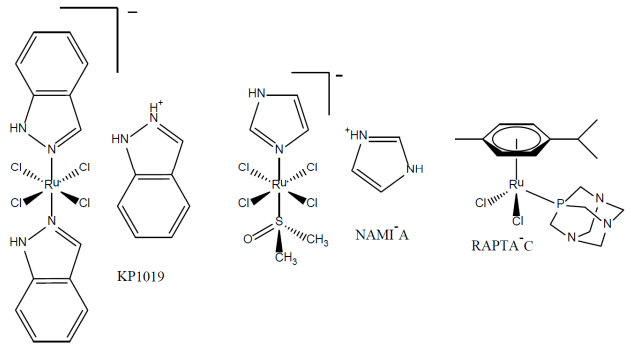

Chart 1. Examples of anti-cancer ruthenium-based agents.

A particularly interesting class of compounds in this regard are the easily accessible half-sandwich ruthenium(II) complexes of the type $[(\eta^6\text{-}C_6H_6)RuCl_2(PR_3)]$ (R = Aryl, O-alky, O-Aryl). Facile reaction of the arene ruthenium dimer $[(\eta^6\text{-}C_6H_6)Ru(\mu\text{-}Cl)Cl]_2$ with strong σ-donor ligands, such as phosphines or phosphites, promote the cleavage of the Ru(II) dimer yielding half-sandwich Ru(II)-arene phosphine complexes [31,32]. A stable phosphine complex, reported in the 1970s $[(\eta^6\text{-}C_6H_6)RuCl_2(PPh_3)]$ [31,32], which is obtained in high yields as a product via a reaction of the afore-mentioned ruthenium dimer with triphenylphosphine. Similarly the phosphite derivatives $[(\eta^6\text{-}C_6H_6)RuCl_2(P(OMe)_3)]$ and $[(\eta^6\text{-}C_6H_6)RuCl_2(P(OPh)_3)]$ are afforded by reaction of $[(\eta^6\text{-}C_6H_6)Ru(\mu\text{-}Cl)Cl]_2$ with trimethyl phosphite and triphenyl phosphite in an analogous fashion [32–34]. Surprisingly, despite the fact that these easily accessible phosphite complexes have been known since the early 1970s, they have not undergone rigorous in vitro cytotoxic testing with respect to cancer cell lines. This encouraged us to prepare and evaluate their cytotoxic activity. Moreover, to the best of our knowledge, the complex $[(\eta^6\text{-}C_6H_6)RuCl_2(P(OPh)_3)]$ has also not been structurally characterised by single crystal X-ray diffraction analysis, which prompted us to carry out such an investigation, and this is also reported herein.

The reaction of half-sandwich ruthenium(II) arene complexes $[(\eta^6\text{-}C_6H_6)RuCl_2(PR_3)]$ (R = aryl or O-Aryl, O-alkyl) with $SnCl_2$ is also known to yield a Ru(II) complex exhibiting a strong covalent Ru-Sn bond via facile insertion of the $SnCl_2$ moiety into the Ru–Cl bond [35,36]. While the reaction of SnX_2 (X = halide) with other metals, such as palladium and platinum, has been extensively studied [37,38], the analogous reaction with ruthenium derivatives has received far less attention. The addition of trichlorostannyl ligands to the coordination sphere of the ruthenium centre is known to enhance the anticancer properties of the complexes from earlier investigations [39], possibly due to the enhanced σ-donor properties of the ligand, which might facilitate and promote the binding of the agent to potential biomolecular targets. Although there is known to be an increase in cytotoxicity, only a few examples of this class, i.e., those bearing stannyl groups, have been tested.

In this work we report the synthesis and characterisation of a series of complexes of formula $[(\eta^6\text{-}C_6H_6)RuX(SnCl_3)(P(OR)_3)]$ (X = Cl, $SnCl_3$ and R = Me, Ph), and some cationic derivatives $[(\eta^6\text{-}C_6H_6)RuX(PPh_3)(DAMP)]BF_4$ (X = $SnCl_3$, Cl), with a view of attempting to delineate the effect of a trichlorostannyl group on cytotoxicity against several cancer cell-lines. Hence, the cytotoxicity of

these new complexes against A2780 and A2780cisR (*cis*-platin resistant) human ovarian carcinoma cells and non-cancerous HEK293 embryonic kidney cells are reported, along with the known complexes $[(\eta^6\text{-}C_6H_6)RuCl_2(PPh_3)]$, $[(\eta^6\text{-}C_6H_6)RuCl_2(P(OPh)_3)]$ and $[(\eta^6\text{-}C_6H_6)RuCl(SnCl_3)(PPh_3)]$, was determined.

2. Results and Discussion

2.1. Synthesis of the Complexes

The reaction of the known complexes $[(\eta^6\text{-}C_6H_6)RuCl_2(P(OX)_3)]$ (X = Me, Ph) with 1.1 equivalents of anhydrous $SnCl_2$ in dichloromethane under reflux affords the complexes $[(\eta^6\text{-}C_6H_6)RuCl(SnCl_3)(P(OX)_3)]$ (X = Me **C1**; X = Ph, **C2**), which were isolated in 64% and 69% yield (Scheme 1), respectively. The reaction of $[(\eta^6\text{-}C_6H_6)Ru(SnCl_3)Cl(P(OMe)_3)]$ with a large excess of $SnCl_2$ in refluxing dichloromethane for 24 h affords the bis-(trichlorostannyl) complex **C3** in 34% yield. The latter complex can also be prepared directly starting from $[(\eta^6\text{-}C_6H_6)RuCl_2(P(OMe)_3)]$ with a 20-fold molar excess of $SnCl_2$ in dichloromethane affording similar yields. Complex **C3**, owing to the presence of an additional $SnCl_3$ moiety is less solubility in dichlormethane or chloroform than **C1** and **C2**, which are highly soluble in these solvents.

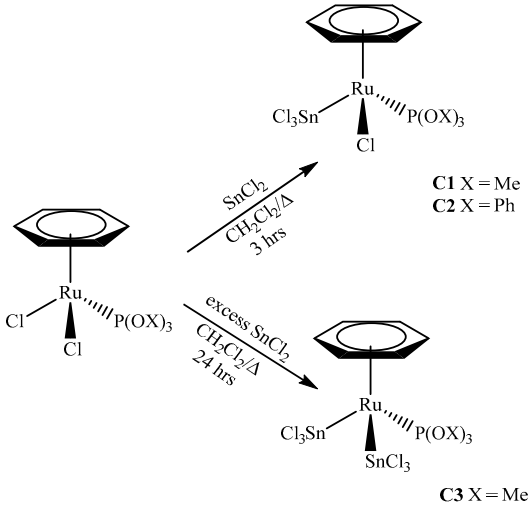

Scheme 1. Synthesis of mono(trichlorostannyl) complexes **C1** and **C2** and di(trichlorostannyl) complex **C3**.

Reaction of $[(\eta^6\text{-}C_6H_6)RuClX(PPh_3)]$ (X = Cl, X= $SnCl_3$) with 1.1 equivalents of 4-dimethylaminopyridine (DMAP) and 1.1 equivalent of ammonium tetrafluoroborate in refluxing methanol affords the complex ionic salts **C4** and **C5** (Scheme 2), both of which are fully characterised by spectroscopic and analytical methods. All complexes **C1**–**C5** exhibit reasonable thermal stability as evidenced by decomposition temperatures in excess of 100 °C.

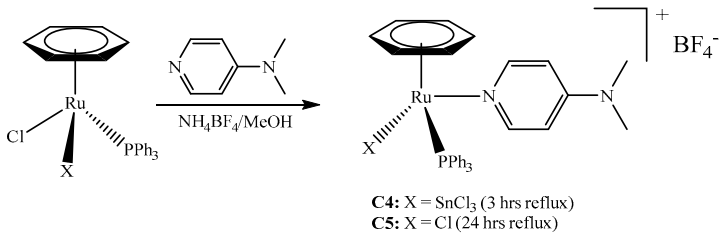

Scheme 2. Synthesis of the cationic complexes **C4** and **C5**.

2.2. Spectroscopic Characterisation

Complexes **C1**–**C3** all exhibit an upfield shifted resonance signal, for the arene protons associated with the η^6-coordinated ring, in the ^{1}H NMR spectra: δ = 6.31 ppm (**C1** and **C3**), 5.82 (**C2**). In complexes **C1** and **C3**, a doublet is observed in the ^{1}H NMR spectrum corresponding to the P(OMe)$_3$ groups due to coupling to the phosphorus atom: ^3J(H,P): **C1**: 12.0 Hz, **C3**: 12.3 Hz.

Complexes **C1**–**C3** exhibit singlet resonance signals in their ^{31}P{^{1}H} NMR spectra: (**C1**: δ = 131.2, **C2**: δ = 122.1, **C3**: δ = 136.5 ppm). Notaby, the presence of both ^{119}Sn and ^{117}Sn satellites, flanking the main resonance signals in all three complexes (**C1**–**C3**) are visible in these spectra due to ^2J(Sn,P) coupling. The presence of the Sn satellites in the ^{31}P{^{1}H} NMR spectra suggest, that in DMSO(dimethyl sulfoxide), the complexes are stable and dynamic $SnCl_3^-$ exchange is unlikely to occur. The formation, in DMSO solutions, of $[(\eta^6\text{-}C_6H_6)Ru(SnCl_3)(DMSO)(PR_3)]^+Cl^-$ can be ruled out for the mono-insertion products **C1** and **C2** over the time periods of the NMR measurements in DMSO-d_6 (12 h). The cationic complexes **C4** and **C5** exibit dramatically shielded chemical shift positions in their respective ^{31}P{^{1}H} NMR spectra (**C4**: δ = 26.7, **C5**: δ = 36.0 ppm) compared with the neutral complexes **C1**–**C3**, owing to their cationic nature. Unfortunately ^{119}Sn NMR spectroscopy could not be carried out on the tin compounds due to the lack of a suitable probe in our laboratories.

The ^{31}P{^{1}H} NMR spectrum of complex **C1** is shown in Figure 1. Both ^{119}Sn and ^{117}Sn satellites are visible, along with rotational side-bands on the main signal, the latter of which is typical in solution ^{31}P NMR spectra.

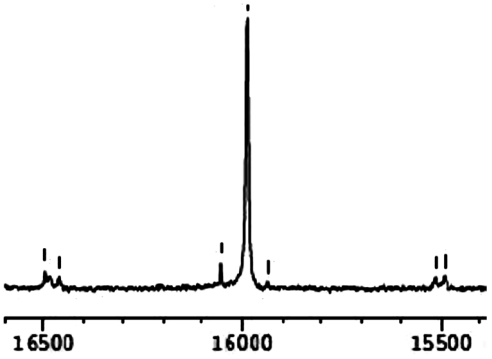

Figure 1. The ^{31}P NMR spectrum of complex **C1** in which the main resonance signal is flanked with ^{117}Sn (inner) and ^{119}Sn (outer) satellites.

Inspection of the experimental solution UV–vis spectra of the complexes **C1**–**C3** reveal that, for the bis-trichlorostannyl complex **C3**, a much higher wavelength of absorption (λ = 459 nm) is observed compared to **C1**: λ = 348 and **C2**: λ = 351 nm, indicating pertubation in the electronic situation upon bis $SnCl_2$-insertion. This is most likely due to the enhanced σ-donor capacity of $SnCl_3^-$ vs. Cl^-. For the ionic complex the UV–vis spectra reveal absorptions at λ = 364 (**C4**) and λ = 335 nm (**C5**), comparable to that of **C1** and **C2**. All complexes were also subjected to a TGA analysis to obtain information on their thermal behaviour and stability. In all cases the complexes are thermally robust with the first onset of mass loss occurring well in excess of 100 °C: (**C1**: 122 °C, **C2**: 186 °C, **C3**: 223 °C, **C4**: 184 °C, and **C5**: 190 °C), which is in accord with the melting point (decomposition temperature) determinations. An exact assignment of the mode of decomposition, i.e., according to which fragments are lost at which temperature was undertaken, and in all cases one decomposition step can be tentatively traced to the loss of the η^6 coordinated ring. Figure 2 shows the TGA trace of complex **C1**. The approximately 12% mass loss can be roughly correlated to the loss of the arene ring.

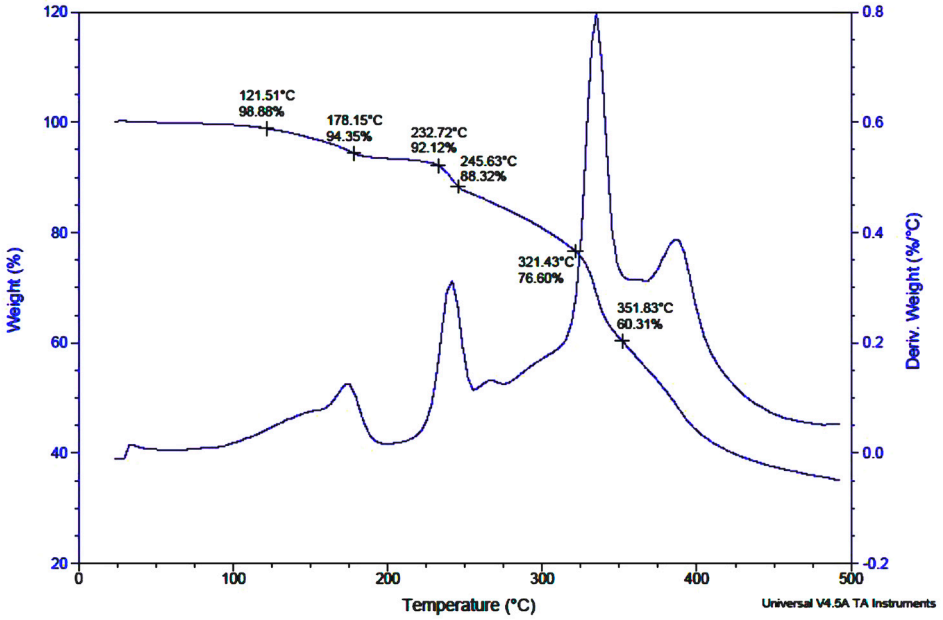

Figure 2. TGA trace of complex **C1** with the onset of decomposition occuring at 121.51 °C.

2.3. X-ray Crystallography

Single crystals of complex **C2** and $[(\eta^6\text{-}C_6H_6)RuCl_2(P(OPh)_3)]$ were obtained and single crystal X-ray diffraction studies were undertaken and their structures are shown in Figures 3 and 4, respectively with selected metric parameters provide in the figure captions (other bond angles and lengths are available in the supporting information). It is somewhat surprising that the complex $[(\eta^6\text{-}C_6H_6)RuCl_2(P(OPh)_3)]$ has eluded structural characterisation by X-ray diffraction, despite being reported in the 1970s.

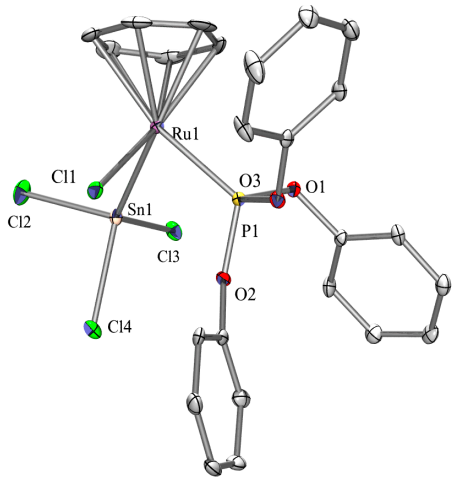

Figure 3. ORTEP view of (**C2**) with atom-labelling scheme and thermal ellipsoids drawn at the 50% probability level. Selected bond distances (Å) and bond angles (°): Ru(1)–Sn(1) = 2.5686(5), Ru(1)–Cl(1) = 2.3919(10), Ru(1)–P(1) = 2.2.242(12). P(1)–Ru(1)–Cl(2) = 90.90(2), P(1)–Ru(1)–Cl(1) = 81.72(2), and Cl(2)–Ru(1)–Cl(1) = 87.49(2).

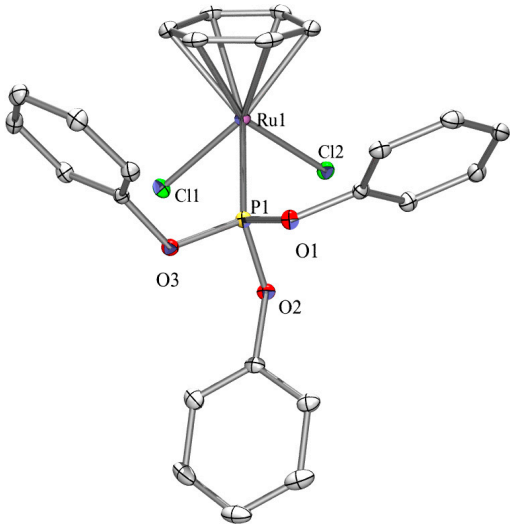

Figure 4. ORTEP view of $[(\eta^6\text{-}C_6H_6)RuCl_2P(OPh)_3]$ with atom-labelling scheme and thermal ellipsoids drawn at the 50% probability level. Selected bond distances (Å) and bond angles (°): C(1)–Ru(1) = 2.191(5), C(2)–Ru(1) = 2.254(5), C(3)–Ru(1) = 2.175(5), C(4)–Ru(1) = 2.246(5), C(5)–Ru(1) = 2.245(5), C(6)–Ru(1) = 2.249(5), C(1–6)–Ru(1)–P(1) = 117.49(18), P(1)–Ru(1)–Cl(1) = 85.71(4), P(1)–Ru(1)–Sn(1) = 86.84(3), and Cl(1)–Ru(1)–Sn(1) = 83.67(3).

Both complexes exhibit the typical piano-stool geometry with the metal centre being coordinated by the arene in η^6 fashion. Complex **C2** exhibits a Ru–Sn bond length of 2.5686(5) Å, which is comparable to known similar complexes featuring Ru–Sn single bonds, for example: $[(\eta^6\text{-}C_6H_6)RuCl(SnCl_3)(PPh)_3]$: 2.5977(14) Å and $[(\eta^6\text{-}p\text{-cymene})RuCl(SnCl_3)(PPh)_3]$: 2.5830(9) Å (see the X-ray structures in Ref. [35]) respectively. Previous structural investigations into complexes of the type $[(\eta^6\text{-}C_6H_6)RuCl_2(PR_3)]$ (R = alkyl, aryl) are ubiquitous, but only three examples of previously structurally-characterised complexes of the type $[(\eta^6\text{-}C_6H_6)RuCl_2(P(OR)_3)]$ (i.e., arene phosphite complexes) exist [40–42] making the structural elucidation of both **C2** and $[(\eta^6\text{-}C_6H_6)RuCl_2P(OPh)_3]$ of some interest.

2.4. Cytotoxicity Studies

The antiproliferative activity of the neutral complexes **C1**–**C3**, cationic complexes **C4** and **C5** and the three known compounds $[(\eta^6\text{-}C_6H_6)RuCl_2(PPh_3)]$, $[(\eta^6\text{-}C_6H_6)RuCl_2(P(OPh)_3)]$, and $[(\eta^6\text{-}C_6H_6)RuCl(SnCl_3)(PPh_3)]$ were investigated in vitro against human ovarian cancer cells A2780 and the A2780cisR variant with aquired *cis*-platin resistance, as well as against non-cancerous human embryonic kidney (HEK293) cells (Table 1). The cytotoxicity of the latter three complexes has not been reported previously and are shown together with *cis*-platin for comparison (Table 2). IC_{50} values of the compounds were determined after exposure of the cells to the compounds for 72 h using the MTT assay.

Complexes **C1** and **C3** with trimethylphosphite ligands did not induce cytotoxicity even at concentrations as high as 500 µM and 200 µM, respectively, whereas all complexes with triphenylphosphite or triphenylphosphine ligands exhibit considerable cytotoxicity in A2780, A2780cisR and HEK293 cells. This is somewhat surprising as the presence of the $SnCl_3$ moiety would have been expected to enhance the cytotoxic effect of the complex (see above). In case of complex **C3**, this may be due to its rather low solubility due to the presence of two trichlorostannyl groups attached to the Ru centre. Notably, the cationic complexes **C4** and **C5** display IC_{50} values in the low micromolar concentration range and, compared to *cis*-platin, showed even high efficacy in A2780cisR cells. Whereas complex **C5** bearing a chloride ligand showed similar activity in all three cell lines, complex **C4** with the chlorine replaced by the $SnCl_3$ moiety, showed slight cancer cell selectivity.

This phenomenon was not observed for $[(\eta^6\text{-}C_6H_6)RuCl_2(PPh_3)]$ and $[(\eta^6\text{-}C_6H_6)RuCl(SnCl_3)(PPh_3)]$, where the tin congener induced generally a two-fold higher cytotoxicity, but did not contribute to cancer cell selectivity. In contrast, the complexes with triphenylphosphite ligands $[(\eta^6\text{-}C_6H_6)RuCl_2(P(OPh)_3)]$ and its tin congener **C2** show the opposite behaviour with **C2** being >20-fold less potent than $[(\eta^6\text{-}C_6H_6)RuCl_2(P(OPh)_3)]$.

Overall looking at these results in totality and attempting to delineate the effect of the trichlorostannyl group on cytotoxicity is not straightforward as obviously solubility plays a key role which might offset the otherwise enhanced cytotoxic activity. Comparison of ionic complexes **C4** and **C5** which have similar solubilities clearly do demonstrate, however, on average, an increase in cytotxicity in the presence of $SnCl_3^-$ vs. Cl^- (except for HEK293). This does suggest that the $SnCl_3^-$ ligand is useful in this regard, but complex **C3**, for example, bearing two $SnCl_3^-$ ligands exhibits very low activity which is driven by its insolubility, thereby potentially offsetting any enhanced efficacy in its cytotoxic effects. We are currently preparing more related complexes to attempt to delineate these effects more closely.

Table 1. In vitro cytotoxicity of complexes against selected tumour cell lines after 72 h drug exposure.

Compound	IC_{50} (μM) [a]		
	A2780	**A2780cisR**	**HEK293**
C1	>500	>500	>500
C2	51.5 ± 0.1	51.5 ± 0.1	25.0 ± 6.2
C3	>200	>200	>200
C4	3.4 ± 0.4	4.1 ± 0.9	14.2 ± 4.9
C5	6.5 ± 0.9	7.1 ± 1.6	3.2 ± 0.3
$[(\eta^6\text{-}C_6H_6)RuCl_2(PPh_3)]$	30.5 ± 0.7	27.0 ± 5.6	27.8 ± 6.8
$[(\eta^6\text{-}C_6H_6)RuCl_2(P(OPh)_3)]$	2.3 ± 0.02	3.2 ± 0.4	1.0 ± 0.5
$[(\eta^6\text{-}C_6H_6)RuCl(SnCl_3)(PPh_3)]$	12.4 ± 0.4	12.5 ± 3.0	4.9 ± 0.1
cis-platin	1.1 ± 0.4	14.4 ± 2.1	10.6 ± 1.4

[a] IC_{50} values (μM) are presented as mean ±SD of two or more independent experiments. The sign (>) indicates that IC_{50} value was not obtained up to given concentration.

3. Experimental

3.1. General Procedures

All manipulations were performed in air as the Ru(II) complexes are stable towards air and moisture. All starting materials and solvents were obtained commercially (Strem, Sigma-Aldrich, Zwijndrecht, Netherlands) and used as received. $[(\eta^6\text{-}C_6H_6)RuCl_2(PPh_3)]$, $[(\eta^6\text{-}C_6H_6)RuCl_2(P(OPh)_3)]$, and $[(\eta^6\text{-}C_6H_6)RuCl(SnCl_3)(PPh_3)]$ were prepared according to published procedures [31–36], and the complexes obtained were characterised by ^1H and ^{31}P NMR spectroscopy and checked against literature data. NMR spectra were recorded on a Bruker Ultrashield 300 (Karlsruhe, Germany), IR spectra on a Shimadzu MIRacle IR (ATR, Kyoto, Japan), UV–vis on a Shimadzu UV 3600 (Kyoto, Japan), and TGA spectra were recorded on a TGA Q-500 (Maastricht, Netherlands) at the University of Maastricht Brightlands Campus, Netherlands. Electrospray (ESI) mass spectrometry experiments were conducted on BRUKER—Ion Trap MS (Karlsruhe, Germany) in positive mode (+) at the University of Neuchâtel, Switzerland. The following abbreviations apply to the intensity of peaks found within the spectra (IR): v: very strong; s: strong; m: medium; and w: weak. For NMR peaks obtained for the non-deuterated residue in the deuterated solvent were used as the internal reference points for the spectra (reference peak: DMSO-d_6, ^1H 2.49 ppm; ^{13}C 39.5 ppm, $CHCl_3$-d_1, ^1H 7.26 ppm; and ^{13}C 77.2 ppm). All signals have been recorded using their appropriate chemical shift (δ in ppm), multiplicity, integral ratio, and coupling constants [Hz]. The following abbreviations apply to the signal multiplicity of peaks within spectra: s = singlet, d = doublet, t = triplet, and m = multiplet.

3.2. Synthesis of the Complexes

3.2.1. Synthesis of [(η^6-C_6H_6)RuCl($SnCl_3$)($P(OMe)_3$)] (**C1**)

[(η^6-C_6H_6)$RuCl_2$($P(OMe)_3$)] (0.500 g, 1.340 mmol) and 1.1 equivalents of anhydrous $SnCl_2$ (0.279 g, 1.474 mmol) were dissolved in 30 mL of dichloromethane and heated under reflux for 3 h. The reaction mixture was cooled to room temperature and filtered to remove excess $SnCl_2$.The bright orange solution was evaporated to dryness in vacuo and afforded a scarlet powder which was subsequently washed with *n*-hexane (3 × 10 mL) and dried under reduced pressure. Yield 64%. m.p.: 103 °C dec. FTIR: v (cm^{-1}): 3075 (w), 2959 (w), 2843 (vw), 1458 (w), 1439 (m), 1260 (m), 1177 (w), 1153 (vw), 1063 (m), 1005 (vs), 922 (w), 866 (w), 791 (vs), 752 (s), 706 (m), 662 (m), 608 (w), 542 (w). ^{1}H NMR: (300.1 MHz, DMSO-d_6, δ, ppm): 6.31 (s, 6H, C_6H_6), 3.82 (d, ^3J(H,P) = 12.0 Hz, 9H, $P(OMe)_3$). ^{13}C NMR: (75.5 MHz, DMSO-d_6, δ, ppm): 92.4 (d, ^2J(C,P) = 3.9 Hz, C_6H_6), 54.7 (d, ^2J(C,P) = 6.2 Hz, $P(OMe)_3$). ^{31}P NMR: (121.5 MHz, DMSO-d_6, δ, ppm): 131.2 (s, $^2J(^{119}Sn,P)$ = 1004.90 Hz; $^2J(^{117}Sn,P)$ = 949.80 Hz). TGA: (Weight % decrease): 121.51–178.15 °C (4.53%), 178.15–232.72 °C (2.23%), 232.72–245.63 °C (3.80%), 245.63–321.43 °C (11.72%) 321.43–351.83 °C (15.77%). UV–vis (nm)/dichloromethane: 347.5, 451.0. EI-MS (CH_3CN): m/z 339.0 $[M - SnCl_3]^+$, 353.4, 381.4, 397.3, 414.9, 426.0, 463.0, 481.0, 522.0, 537.0, 554.6, 582.7 $[M + Na]^+$ (other higher mass unassignable fragments present).

3.2.2. Synthesis of [(η^6-C_6H_6)RuCl($SnCl_3$)($P(OPh)_3$)] (**C2**)

Complex (**C2**) was synthesized in an analogous fashion as for (**C1**) starting from [(η^6-C_6H_6)$RuCl_2$($P(OPh)_3$)]: (0.500 g, 0.892 mmol) and $SnCl_2$ (0.186 g, 0.981 mmol). Bright-orange crystals. Yield 69%. m.p.: 197 °C dec. FTIR: v (cm^{-1}): 3075 (vw), 296 3(vw), 1583 (m), 1481 (s), 1437 (w), 1260 (w), 1206 (m), 1182 (s), 1173 (s), 1152 (s), 1022 (m), 945 (s), 922 (s), 908 (s), 891 (s), 822 (vs), 800 (m), 766 (vs), 688 (s), 601 (m). ^{1}H NMR: (300.1 MHz, DMSO-d_6, δ, ppm): 7.50 (d, ^3J(H,H) = 7.4 Hz, 6H, $P(OPh_3)$), 7.35 (d, ^3J(H,H) = 7.4 Hz, 3H, $P(OPh)_3$), 7.34 (br s, 6H, $P(OPh)_3$), 5.84 (br s, 6H, C_6H_6), ^{13}C NMR: (75.5 MHz, DMSO-d_6, δ, ppm): 151.0 (d, ^1J(C,P)= 10.8 Hz, C^1, $P(OPh)_3$), 130.5 (s, $C^{2,6}$, $P(OPh)_3$), 126.4 (s, C^4, $P(OPh)_3$), 121.9 (d, ^xJ(C,P) = 4.2 Hz, $C^{3,5}$, $P(OPh)_3$), 92.9 (d, ^2J(C,P) = 3.8 Hz, C_6H_6), ^{31}P NMR: (300.1 MHz, DMSO-d_6, δ, ppm): 122.1 (s, $^3J(^{119}Sn,P)$ = 989.0 Hz, $^2J(^{117}Sn,P)$ = 946.6 Hz). TGA: (Weight % decrease): 185.99–202.83 °C (4.52%), 202.83–347.70 °C (18.50%), 347.70–393.60 °C (30.06%). UV–vis (nm)/dichloromethane: 351.1, 453.0. ESI–MS (CH_3CN/MeOH): m/z 123.2, 353.4, 381.4, 449.3, 516.5, 599.1, 683.4, 711.0, 739.0, 767.7 $[M + Na]^+$ (other higher mass fragments present).

3.2.3. Synthesis of [(η^6-C_6H_6)Ru($SnCl_3$)$_2$($P(OMe)_3$)] (**C3**)

The complex **C1** was weighed into a flask (0.900 g, 1.200 mmol) along with a twenty-fold molar excess of $SnCl_2$ (4.560 g, 24.000 mmol) in dichloromethane (100 mL) and refluxed for 20 h. During this time the reaction turned a lemon-yellow colour. The reaction solution was filtered to remove unreacted $SnCl_2$ and the solvent of the filtrate removed in vacuo affording a pineapple-yellow waxy solid, which was washed with Et_2O (3 × 10 mL) and the washings discarded. The compound can also be prepared directly from [η^6-(C_6H_6)$RuCl_2$($P(OMe)_3$)] with addition of a large excess of $SnCl_2$ (20 molar equiv.) in dichloromethane with reflux for 24 h and isolation as describe above. Yield 34%. m.p.: 146 °C dec. Conductivity (DMSO): (μS·cm^{-1}, 21 °C, 0.5 mg·mL^{-1}): 0.2. FTIR: v (cm^{-1}): 3078 (vw), 2961 (vw), 1441 (w), 1260 (m), 1173 (w), 1088 (m), 1009 (vs), 922 (w), 864 (w), 787 (vs), 733 (s), 704 (m), 662 (w), 648 (w), 608 (vw), 561 (w). ^{1}H NMR: (300.1 MHz, DMSO-d_6, δ, ppm): 6.31 (br s, 6H, C_6H_6), 3.72 (d, ^3J(H,P) = 12.3 Hz, 9H, $P(OMe)_3$), ^{13}C NMR: (75.5 MHz, DMSO-d_6, δ, ppm): 94.0 (d, ^2J(C,P) = 4.1 Hz, C_6H_6), 54.5 (d, ^2J(C,P) = 6.6 Hz, $P(OMe)_3$), ^{31}P NMR: (121.5 MHz, DMSO-d_6, δ, ppm): 136.5 (s, $^2J(^{119}Sn,P)$ = 741.7 Hz; $^2J(^{117}Sn,P)$ = 722.1 Hz). TGA: (Weight % decrease): 223.14–273.12 °C (12.70%), 273.12–317.27 °C (2.02%), 317.27–336.42 °C (11.56%), 336.42–394.73 °C (31.77%). UV–vis: (nm)/dichloromethane: 459. ESI–MS (CH_3CN/MeOH): m/z 477.3, 541.2, 610.2, 615.2, 631.1, 684.2,

689.1, 698.6, 705.1, 718.5, 747.0, 758.2, 779.1 $[M + Na]^+$ (other higher mass unassignable fragments also present).

3.2.4. Synthesis of $[(\eta^6\text{-}C_6H_6)Ru(SnCl_3)(PPh_3)(DMAP)]^+BF_4^-$ (**C4**)

$[(\eta^6\text{-}C_6H_6)RuCl(SnCl_3)(PPh_3)]$ (0.30 g, 0.60 mmol) in 25 mL of methanol was stirred for ca. 5 min. 1.1 molar equivalents of 4-dimethylaminopyridine (DMAP) (0.060 g, 0.66 mmol) was added to the mixture and stirred for 30 min and 1.1 equivalent of ammonium tetrafluoroborate (0.05 g, 0.66 mmol) was added to the solution and the mixture heated at reflux overnight. The distinct orange solution was evaporated to dryness and afforded a dark red powder, which was subsequently washed with *n*-hexane and dried under reduced pressure. Yield 96%. m.p.: 119 °C dec. FTIR: v (cm^{-1}): 3479 (w), 3317 (w), 3055 (w), 2960 (w), 2823 (w), 1647 (m), 1616 (w), 1560 (m), 1480 (w), 1433 (m), 1419 (m), 1404 (m), 1250 (m), 1217 (m), 1186 (w), 1087 (s), 1060 (s), 1026 (vs), 997 (m), 941 (w), 819 (m), 798 (s), 748 (s), 723 (m), 696 (s), 659 (m). ^{1}H NMR: (300.1 MHz, $CDCl_3$, δ, ppm): 8.02 (br s, 2H, $C_5H_4N(N(CH_3)_2)$) 7.77-7.38 (m, 15H, PPh_3), 6.76 (br s, 2H, $C_5H_4N(N(CH_3)_2)$, 5.40 (s, 6H, C_6H_6), 3.25 (s, 6H, $N(CH_3)_2$). ^{13}C NMR: (75.5 MHz, $CDCl_3$, δ, ppm): (low field signals expected for DMAP not visible, nor C^1 of PPh_3), 134.2 (d, ^xJ(C,P) = 10.7 Hz, $C^{2,6}$, PPh_3) 131.0 (br s, C^4, PPh_3), 128.2 (d, ^xJ(C,P) = 9.6 Hz, $C^{3,5}$, PPh_3), 106.9 (s, $C_5H_4N(N(CH_3)_2)$, 89.2 (d, ^2J(C,P) = 3.6 Hz, C_6H_6), 40.3 (s, $N(CH_3)_2$). ^{31}P NMR: (121.5 MHz, $CDCl_3$, δ, ppm): 26.7 (s). TGA: (Weight % decrease): 183.46–242.84 °C (5.7%), 242.84–277.79 °C (4.77%), 277.79–337.59 °C (26.75%), 337.59–404.13 °C (18.85%). UV–vis: (nm)/dichloromethane: 364.5. ESI–MS (CH_3CN): m/z 123.2 $[DMAP + H]^+$, 401.1, 479.0, 599.1, 635.0, 738.0, 785.0 (other unassignable higher mass fragments also present).

3.2.5. Synthesis of $[(\eta^6\text{-}C_6H_6)RuCl(PPh_3)(DMAP)]^+BF_4^-$ (**C5**)

Complex (**C5**) was synthesized in an analogous fashion as (**C4**), except $[(\eta^6\text{-}C_6H_6)RuCl_2(PPh_3)]$ was used as starting material. The work up and isolation procedure is analogous. Yield 24%. m.p.: 176 °C dec. FTIR: v (cm^{-1}): 2898 (w), 2983 (w), 1622 (m), 1614 (m), 1588 (m), 1537 (m), 1481 (m), 1435 (m), 1406 (m), 1386 (m), 1230 (m), 1089 (s), 1055 (vs), 1018 (vs), 999 (s), 808 (m), 748 (s), 694 (vs). ^{1}H NMR: (300.1 MHz, $CDCl_3$, δ, ppm): 8.21 (d, ^3J(H,H) = 6.1 Hz, $C_5H_4N(N(CH_3)_2)$), 7.38–7.73 (m, 15H, PPh_3), 6.26 (d, ^3J(H,H) = 6.21 Hz, $C_5H_4N(N(CH_3)_2)$), 5.76 (s, 6H, C_6H_6), 2.94 (s, 6H, $N(CH_3)_2$). ^{13}C NMR: (75.5 MHz, $CDCl_3$, δ, ppm): (low field signals expected for DMAP not visible), 154.5 (s, C^1, PPh_3), 133.8 (d, ^xJ(C,P) = 10.5, $C^{2,6}$, PPh_3), 131.1 (br s, C^4, PPh_3), 128.8 (d, ^xJ(C,P) = 9.6, $C^{3,5}$, PPh_3), 108.3 (s, $C_5H_4N(N(CH_3)_2)$, 90.5 (d, ^2J(C,P) = 3.0 Hz, C_6H_6), 39.1 (s, $C_5H_4N(N(CH_3)_2)$). ^{31}P NMR: (121.5 MHz, $CDCl_3$, δ, ppm): 36.0. TGA: (Weight % decrease): 190.65–214.81 °C (12.58%), 214.81–263.54 °C(11.91%), 263.54–273.12 °C (3.86%), 273.12–398.48 °C (16.12%). UV–vis: (nm)/dichloromethane: 335.0. ESI–MS (CH_3CN): m/z 477.0, 553.0, 599.0 $[M - BF_4]^+$ (no other fragments visible).

3.3. Crystallographic Structure Determination

Crystals of X-ray diffraction quality were obtained by slow evaporation of a dichloromethane-diethyl ether 1:1 mixture of (**C2**) and $[(\eta^6\text{-}C_6H_6)RuCl_2(P(OPh)_3)]$ at room temperature using a vial with a narrow opening. For X-ray structure analyses the crystals are mounted onto the tip of glass fibers, and data collection was performed with a BRUKER-AXS SMART APEX CCD diffractometer using graphite-monochromated Mo Kα radiation (0.71073 Å) (Table 2). The data were reduced to F_o^2 and corrected for absorption effects with SAINT [43] and SADABS [44,45], respectively. The structures were solved by direct methods and refined by full-matrix least-squares method (*SHELXL97*) [46]. If not noted otherwise all non-hydrogen atoms were refined with anisotropic displacement parameters. All hydrogen atoms were located in calculated positions to correspond to standard bond lengths and angles. All diagrams are drawn with 30% probability thermal ellipsoids and all hydrogen atoms were omitted for clarity. Figures of solid state molecular structures were generated using Ortep-3 as implemented in WINGX [47] and rendered using POV-ray 3.6 [48].

Table 2. Crystal data, details of data collection and structure refinement parameters for (**C2**) and [(η^6-C_6H_6)$RuCl_2${$P(OPh)_3$}].

Complex	C2	[(η^6-C_6H_6)$RuCl_2${$P(OPh)_3$}]
Empirical formula	$C_{24}H_{21}Cl_4PRuSn$	$C_{24}H_{21}Cl_2O_3PRu$
Formula weight	749.94	560.35
T/K	100(2) K	446(2) K
λ/Å Crystal system	0.71073 Orthorhombic	0.71073 Orthorhombic
Space group	P2(1)2(1)2(1)	Pbca
a/Å	8.7164(17)	17.371(3)
b/Å	16.420(3)	14.997(3)
c/Å	18.514(4)	17.551(3)
α(deg.)	90	90
β(deg.)	90	90
γ(deg.)	90	90
V(Å^3)	2649.9(9)	4572.6(14)
Z	4	8
Density$_{calc}$(mg·m^{-3})	1.880	1.628
Absorption coefficient (mm^{-1})	2.001	1.013
F(000)	1464	2256
Crystal size (mm)	0.42 × 0.08 × 0.06	0.38 × 0.36 × 0.16
Theta range for data collection (deg.)	1.66–26.33	2.14–26.34
Limiting indices	$-10 \leq h \leq 10$, $-16 \leq k \leq 20$, $-23 \leq l \leq 23$	$-21 \leq h \leq 21$, $-18 \leq k \leq 18$, $-21 \leq l \leq 21$
Reflections Collected/Unique	17168/5368 [R(int) = 0.0409]	34691/4657 [R(int) = 0.0339]
Completeness of theta max.	26.33 (99.6%)	26.34 (99.9%)
Absorption correction	SADABS	SADABS
Refinement method	Full-matrix least-squares on F^2	Full-matrix least-squares on F^2
Data/Restraints/Parameters	5368/0/308	4657/0/280
Goodness-of-fit on F^2 (GOF)	1.042	1.117
Largest diff. peak and hole (e·Å^{-3})	0.805 and −0.471	0.566 and −0.404

3.4. Cell Cultures and Cytotoxicity Measurements

Human A2780 and A2780cisR ovarian carcinoma cells were obtained from the European Collection of Authenticated Cell Cultures (ECACC, Salisbury, UK) and non-cancerous HEK293 cells were obtained from ATCC (Sigma, St. Gallen, Switzerland). A2780 were routinely grown in RPMI (Roswell Park Memorial Institute) medium: 1640 GlutaMAX (Lifetechnologies, Zug, Switzerland), while HEK293 were maintained in DMEM medium (Dulbecco's modified media), both containing 10% heat-inactivated fetal bovine serum (FBS, Pan Biotech, Aidenbach, Germany) and 1% antibiotics (penicillin/streptomycin), at a humidified atmosphere with 5% CO_2 at 37 °C. Cytotoxicity was determined using the MTT assay (MTT = 3-(4,5-dimethyl-2-thiazolyl)-2,5-diphenyl-2*H*-tetrazolium bromide). Cells were seeded in 96-well plates as monolayers with 100 µL of cell solution per well and were pre-incubated for 24 h in the cell culture medium. Compounds were prepared as DMSO stock solutions that were dissolved in the culture medium and two-fold serially diluted to the appropriate concentration to give a final DMSO concentration of maximum 0.5%. 100 µL of the compound solution were added to each well and the plates were incubated for 72 h. Subsequently, MTT (5 mg/mL solution, 20 µL per well) was added to the cells and the plates were incubated for another 4 h. The culture medium was aspirated, and the purple formazan crystals formed by the mitochondrial dehydrogenase activity of vital cells were dissolved in DMSO (100 µL). The optical density, directly proportional to the number of surviving cells, was quantified at 590 nm using a multiwell plate reader (Molecular Devices). The fraction of surviving cells was calculated from the absorbance of untreated control cells. The IC_{50} values for the inhibition of cell growth were determined by fitting the plot of the logarithmic percentage of surviving cells against the logarithm of the drug concentration using a linear regression function. Evaluation is based on means (±SD) from at least two independent experiments, each comprising four tests per concentration level.

4. Conclusions

A series of novel, neutral, and cationic η^6-arene ruthenium(II) complexes, some bearing one or two trichlorostannyl groups, have been synthesized, characterized, and tested in vitro for antiproliferative activity against human ovarian cancer cells and a non-tumorigenic cell line. Complexes **C1** and **C3**

exhibit rather poor cyctotoxic activity, whilst complex **C2** exhibits moderate activity. The lack of potency of complexes **C1** and **C3** may be linked to solubility in aqueous media, despite the presence of stannyl ligands expected to enhance the cytotoxicity. The ionic complexes **C4** and **C5** are cytotoxic, with an activity similar to *cis*-platin, with **C4** even showing a degree of cancer cell selectivity. We are currently attempting to further delineate the effect of the $SnCl_3^-$ moiety on related complexes, taking solubility into consideration, and will report these endeavours in due course.

Supplementary Materials: The following are available online at www.mdpi.com/2304-6740/5/3/44/s1, A PDF document with the details of the X-ray crystallographic analysis is available. Crystallographic data (excluding structure factors) for the structures of compounds (**C2**) and [(η^6-C_6H_6)$RuCl_2$(P($OPh)_3$)] reported in this paper are deposited with the Cambridge Crystallographic Data Center as supplementary publication no. CCDC-1555463 (**C2**) and 1555464 ([(η^6-C_6H_6)$RuCl_2$(P($OPh)_3$)]). Copies of data can be obtained free of charge at: http://www.ccdc.cam.ac.uk/products/csd/request/.

Acknowledgments: Burgert Blom thanks the Maastricht Science Programme and Maastricht University for support in carrying out this research. Bruno Therrien (Université de Neuchâtel) is gratefully acknowledged for submitting samples for mass spectrometry on the complexes and for very useful discussions and suggestions during the preparation of the manuscript.

Author Contributions: Olivier Renier, Connor Deacon-Price, Joannes E. B. Peters, Kunsulu Nurekeyeva, Catherine Russon, Simba Dyson: Carried out the synthesis and characterisation. Siyabonga Ngubane, Haleden Chiririwa: Assisted with interpretation of data and writing. Judith Baumgartner: X-ray structural investigations. Paul J. Dyson, Tina Riedel: Performed cytotoxic testing and wrote that part of the manuscript. Burgert Blom: Initiated, coordinated and supervised research, wrote most of the manuscript except cytotoxic part, corresponding author.

Conflicts of Interest: The authors declare no conflict of interest.

References

1. Rosenberg, B.; Vancamp, L. Platinum compounds: A new class of potent antitumour agents. *Nature* **1969**, *222*, 385–386. [CrossRef] [PubMed]
2. Lippman, A.J.; Helson, C.; Helson, L.; Krakoff, I.H. Clinical trials of *cis*-diamminedichloroplatinum (nsc-119875). *Cancer Chemother. Rep.* **1973**, *57*, 191–200. [PubMed]
3. Siddik, Z.H. Cisplatin: Mode of cytotoxic action and molecular basis of resistance. *Oncogene* **2003**, *22*, 7265–7279. [CrossRef] [PubMed]
4. Galanski, M.; Jakupec, M.A.; Keppler, B.K. Update of the preclinical situation of anticancer platinum complexes: Novel design strategies and innovative analytical approaches. *Curr. Med. Chem.* **2005**, *12*, 2075–2094. [CrossRef] [PubMed]
5. Abid, M.; Shamsi, F.; Azam, A. Ruthenium complexes: An emerging ground to the development of metallopharmaceuticals for cancer therapy. *Mini Rev. Med. Chem.* **2016**, *16*, 772–786. [CrossRef] [PubMed]
6. Ott, I.; Gust, R. Non Platinum Metal Complexes as Anti-cancer Drugs. *Arch. Der Pharm.* **2007**, *340*, 117–126. [CrossRef] [PubMed]
7. Momekov, G.; Bakalova, A.; Karaivanova, M. Novel approaches towards development of non-classical platinum-based antineoplastic agents: Design of platinum complexes characterized by an alternative DNA-binding pattern and/or tumor-targeted cytotoxicity. *Curr. Med. Chem.* **2005**, *12*, 2177–2191. [CrossRef] [PubMed]
8. Xin Zhang, C.; Lippard, S. New metal complexes as potential therapeutics. *Curr. Opin. Chem. Biol.* **2003**, *7*, 481–489.
9. Wu, Q.; Fan, C.; Chen, T.; Liu, C.; Mei, W.; Chen, S.; Wang, B.; Chen, Y.; Zheng, W. Microwave-assisted synthesis of arene ruthenium(II) complexes that induce *s*-phase arrest in cancer cells by DNA damage-mediated p53 phosphorylation. *Eur. J. Med. Chem.* **2013**, *63*, 57–63. [CrossRef] [PubMed]
10. Sava, G.; Bergamo, A. Ruthenium-based compounds and tumour growth control. *Int. J. Oncol.* **2000**, *17*, 353–418. [CrossRef] [PubMed]
11. Sava, G.; Bergamo, A. Ruthenium Drugs for Cancer Chemotherapy: An Ongoing Challenge to Treat Solid Tumours. In *Platinum and Other Heavy Metal Compounds in Cancer Chemotherapy: Molecular Mechanisms and Clinical Applications*; Bonetti, A., Leone, R., Muggia, F.M., Howell, S.B., Eds.; Humana Press: Totowa, NJ, USA, 2009; pp. 57–66.

12. Barry, N.P.; Sadler, P.J. 100 Years of metal coordination chemistry: From Alfred Werner to anticancer metallodrugs. *Pure Appl. Chem.* **2014**, *86*, 1897–1910. [CrossRef]
13. Mjos, K.D.; Orvig, C. Metallodrugs in medicinal inorganic chemistry. *Chem. Rev.* **2014**, *114*, 4540–4563. [CrossRef] [PubMed]
14. Esteban Leon, I.; Fernando Cadavid-Vargas, J.; Laura Di Virgilio, A.; Beatriz Etcheverry, S. Vanadium, ruthenium and copper compounds: A new class of nonplatinum metallodrugs with anticancer activity. *Curr. Med. Chem.* **2017**, *24*, 112–148. [CrossRef] [PubMed]
15. Brabec, V.; Hrabina, O.; Kasparkova, J. Cytotoxic platinum coordination compounds. DNA binding agents. *Coord. Chem. Rev.*. In Press. [CrossRef]
16. Hartinger, C.G.; Jakupec, M.A.; Zorbas-Seifried, S.; Groessl, M.; Egger, A.; Berger, W.; Zorbas, H.; Dyson, P.J.; Keppler, B.K. Kp1019, a new redox-active anticancer agent-preclinical development and results of a clinical phase I study in tumor patients. *Chem. Biodivers.* **2008**, *5*, 2140–2155. [CrossRef] [PubMed]
17. Hartinger, C.G.; Zorbas-Seifried, S.; Jakupec, M.A.; Kynast, B.; Zorbas, H.; Keppler, B.K. From bench to bedside—Preclinical and early clinical development of the anticancer agent indazolium *trans*-[tetrachlorobis(1*H*-indazole)ruthenate(III)] (kp1019 or ffc14a). *J. Inorg. Biochem.* **2005**, *100*, 891–904. [CrossRef] [PubMed]
18. Pettinari, R.; Petrini, A.; Marchetti, F.; Pettinari, C.; Riedel, T.; Therrien, B.; Dyson, P.J. Arene-ruthenium(II) complexes with bioactive *ortho*-hydroxydibenzoylmethane ligands: Synthesis, structure, and cytotoxicity. *Eur. J. Inorg. Chem.* **2017**, *12*, 1800–1806. [CrossRef]
19. Scolaro, C.; Geldbach, T.J.; Rochat, S.; Dorcier, A.; Gossens, C.; Bergamo, A.; Cocchietto, M.; Tavernelli, I.; Sava, G.; Rothlisberger, U.; et al. Influence of Hydrogen-Bonding Substituents on the Cytotoxicity of RAPTA Compounds. *Organometallics* **2006**, *25*, 756–765. [CrossRef]
20. Scolaro, C.; Chaplin, A.B.; Hartinger, C.G.; Bergamo, A.; Cocchietto, M.; Keppler, B.K.; Sava, G.; Dyson, P.J. Tuning the hydrophobicity of ruthenium(II)-arene (RAPTA) drugs to modify uptake, biomolecular interactions and efficacy. *Dalton Trans.* **2007**, *43*, 5065–5072. [CrossRef] [PubMed]
21. Scolaro, C.; Bergamo, A.; Brescacin, L.; Delfino, R.; Cocchietto, M.; Laurenczy, G.; Sava, G.; Dyson, P.J. In Vitro and In Vivo Evaluation of Ruthenium(II)-Arene PTA Complexes. *J. Med. Chem.* **2005**, *48*, 4161–4171. [CrossRef] [PubMed]
22. Weiss, A.; Ding, X.; van Beijnum, J.R.; Wong, I.; Wong, T.J.; Berndsen, R.H.; Dormond, O.; Dallinga, M.; Shen, L.; Schingemann, R.O.; et al. Rapid optimization of drug combinations for the optimal angiostatic treatment of cancer. *Angiogenesis* **2015**, *18*, 233–244. [CrossRef] [PubMed]
23. Allardyce, C.S.; Dyson, P.J.; Ellis, D.J.; Heath, S.L. [Ru(η-cymene)Cl(PTA)] (PTA = 1,3,5-triaza-7-phosphatricyclo-[3.3.1.1]decane): A water soluble compound that exhibits pH dependent DNA binding providing selectivity for diseased cells. *Chem. Commun.* **2001**, *15*, 1396–1397. [CrossRef]
24. Pettinari, R.; Marchetti, F.; Petrini, A.; Pettinari, C.; Lupidi, G.; Fernández, B.; Diéguez, A.R.; Santoni, G.; Nabissi, M. Ruthenium(II)-arene complexes with dibenzoylmethane induce apoptotic cell death in multiple myeloma cell lines. *Inorg. Chim. Acta* **2017**, *454*, 139–148. [CrossRef]
25. Kurzwernhart, A.; Kandioller, W.; Enyedy, É.A.; Novak, M.; Jakupec, M.A.; Keppler, B.K.; Hartinger, C.G. 3-hydroxyflavones vs. 3-hydroxyquinolinones: Structure–activity relationships and stability studies on Ru(II) (arene) anticancer complexes with biologically active ligands. *Dalton Trans.* **2013**, *42*, 6193–6202. [CrossRef] [PubMed]
26. Singh, A.K.; Pandey, D.S.; Xu, Q.; Braunstein, P. Recent advances in supramolecular and biological aspects of arene ruthenium (II) complexes. *Coord. Chem. Rev.* **2014**, *270*, 31–56. [CrossRef]
27. Betanzos-Lara, S.; Liu, Z.; Habtemariam, A.; Pizarro, A.M.; Qamar, B.; Sadler, P.J. Organometallic ruthenium and iridium transfer-hydrogenation catalysts using coenzyme NADH as a cofactor. *Angew. Chem. Int. Ed.* **2012**, *51*, 3897–3900. [CrossRef] [PubMed]
28. Carrión, M.C.; Sepúlveda, F.; Jalón, F.A.; Manzano, B.R.; Rodríguez, A.M. Arene-ruthenium (II) complexes containing bispyrazolylmethane ligands: Effect of the ligand substituents on the formation of an isomer and on the fluxional behaviour. *Eur. J. Inorg. Chem.* **2013**, 217–227. [CrossRef]
29. Singh, S.K.; Pandey, D.S. Multifaceted half-sandwich arene-ruthenium complexes: Interactions with biomolecules, photoactivation, and multinuclearity approach. *RSC Adv.* **2014**, *4*, 1819–1840. [CrossRef]
30. Therrien, B. Functionalised η^6-arene ruthenium complexes. *Coord. Chem. Rev.* **2009**, *253*, 493–519. [CrossRef]

31. Robertson, D.R.; Stephenson, T.; Arthur, T. Cationic, neutral and anionic complexes of ruthenium(II) containing η^6-arene ligands. *J. Organomet. Chem.* **1978**, *162*, 121–136. [CrossRef]
32. Zelonka, R.A.; Baird, M.C. Benzene complexes of ruthenium(II). *Can. J. Chem.* **1972**, *50*, 3063–3072. [CrossRef]
33. Zelonka, R.; Baird, M. Reactions of π-benzeneruthenium(II) complexes with alkylating reagents. *J. Organomet. Chem.* **1972**, *44*, 383–389. [CrossRef]
34. Bennett, M.A.; Smith, A.K. Arene ruthenium(II) complexes formed by dehydrogenation of cyclohexadienes with ruthenium (III) trichloride. *J. Chem. Soc. Dalton Trans.* **1974**, *2*, 233–241. [CrossRef]
35. Therrien, B.; Thai, T.-T.; Freudenreich, J.; Süss-Fink, G.; Shapovalov, S.S.; Pasynskii, A.A.; Plasseraud, L. Bimetallic ruthenium–tin chemistry: Synthesis and molecular structure of arene ruthenium complexes containing trichlorostannyl ligands. *J. Organomet. Chem.* **2010**, *695*, 409–414. [CrossRef]
36. Novák, M.; Bouška, M.; Dostál, L.; Lutter, M.; Jurkschat, K.; Turek, J.; De Proft, F.; Růžičková, Z.; Jambor, R. Role of the trichlorostannyl ligand in tin–ruthenium arene complexes: Experimental and computational studies. *Eur. J. Inorg. Chem.* **2017**, *2017*, 1292–1300. [CrossRef]
37. Thoonen, S.H.; Lutz, M.; Spek, A.L.; Deelman, B.-J.; van Koten, G. Synthesis of novel trialkyl (trichlorostannyl) platinum(IV) complexes through $SnCl_2$ insertion into the Pt–Cl bond. *Organometallics* **2003**, *22*, 1156–1159. [CrossRef]
38. Blom, B. Reactivity of Ylenes at Late Transition Metal Centres. Ph.D. Thesis, Bonn University, Bonn, Germany, 2011.
39. Gras, M.; Therrien, B.; Süss-Fink, G.; Casini, A.; Edafe, F.; Dyson, P.J. Anticancer activity of new organo-ruthenium, rhodium and iridium complexes containing the 2-(pyridine-2-yl) thiazole *N*,*N*-chelating ligand. *J. Organomet. Chem.* **2010**, *695*, 1119–1125. [CrossRef]
40. Joslin, E.E.; McMullin, C.L.; Gunnoe, T.B.; Cundari, T.R.; Sabat, M.; Myers, W.H. Coordination chemistry of 4-methyl-2,6,7-trioxa-1-phosphabicyclo[2,2,1]heptane: Preparation and characterization of Ru(II) complexes. *Inorg. Chem.* **2012**, *51*, 4791–4801. [CrossRef] [PubMed]
41. Meijboom, R.; Muller, A.; Roodt, A. (η^6-Benzene)dichloro[tris(2-isopropylphenyl) phosphite]ruthenium(II) dichloromethane solvate. *Acta Crystallogr. Sect. E* **2006**, *62*, m1866–m1868. [CrossRef]
42. Fernandez-Zumel, M.A.; Lastra-Barreira, B.; Scheele, M.; Diez, J.; Crochet, P.; Gimeno, J. Chiral phosphonite, phosphite and phosphoramidite η^6-arene-ruthenium(II) complexes: Application to the kinetic resolution of allylic alcohols. *Dalton Trans.* **2010**, *39*, 7780–7785. [CrossRef] [PubMed]
43. *SAINTPLUS: Software Reference Manual*; Version 6.45; Bruker-AXS: Madison, WI, USA, 1997–2003.
44. Blessing, R. An empirical correction for absorption anisotropy. *Acta Crystallogr. Sect. A* **1995**, *51*, 33–38. [CrossRef]
45. Sheldrick, G.M. *SADABS*; Version 2.10; Bruker-AXS Inc.: Madison, WI, USA, 2003.
46. Sheldrick, G. A short history of *SHELX*. *Acta Crystallogr. Sect. A* **2008**, *64*, 112–122. [CrossRef] [PubMed]
47. Farrugia, L. WinGX and ORTEP for Windows: An update. *J. Appl. Crystallogr.* **2012**, *45*, 849–854. [CrossRef]
48. POVRAY 3.6. Persistence of Vision Pty. Ltd.: Williamstown, Victoria, Australia, 2004. Available online: http://www.povray.org/download/ (accessed on 9 July 2008).